Model Identifying the Airfoilicing Process Beginning on the Basis of Aircraft Flight Parameters

Damian Olejniczak[0000-0002-5144-8396] and *Marcin* Nowacki[0000-0003-4347-9392]

Poznan, Poland Poznan University of Technology, Institute of Machine Design, Faculty of Mechanical Engineering, Piotrowo 3, 60-965 Poznań, Poland

Abstract. Aircraft icing is the process of changing the state of concentration of water contained in the air in the form of steam into a solid form accumulating on the surface of aircraft construction elements during a flight or results from the direct accumulating of ice crystals on the aircraft surface. The process of aircraft icing is complex and depends on many variable factors related to atmospheric conditions and aircraft flight parameters. The goal of work is to develop a deterministic model for identifying the beginning of the icing process depending on the aircraft flight parameters on the basis of CFD simulations.

1 Introduction

The casting Aerodynes stay in the air thanks to two forces: the thrust force F_T produced by the aircraft enginesrequired to cause object movement and the lift force F_L generated as a result of the flow of the medium relative to the wing airfoil. Lift force F_L is a component of aerodynamic force F_A.According to the principle of energy conservation and the equation of flow continuity, when the wing moves relative to the medium, a pressure gradient is generated between the lower and upper airfoil boundary layers of the flow, as a result, is created a lift force F_L, whose vector is perpendicular to the direction of motion.The second component of aerodynamic force $F_A$is the drag force F_D, parallel and directed against the direction of body movement (fig. 1) [1].

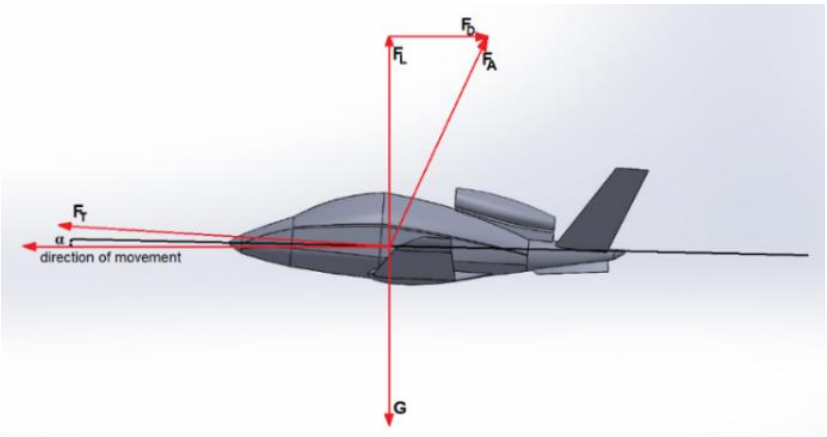

Fig. 1. Forces affecting the aircraft during horizontal flight: G – gravity force, F_T – thrust force, F_A – total aerodynamic force, F_L – lift force, F_D – drag force, α – angle of attack.

The phenomenon of aircraft icing is the process of changing the state of concentration of water contained in the air in the form of water vapor to a solid form deposited on the surface of aircraft construction elements or direct deposition on the surface of the ice crystals [2, 3].

The icing occurs under atmospheric conditions conducive to the phenomenon, which include:

- high air humidity,
- air temperature from 0°C to –40°C,
- the presence of water in the atmosphere in the form of supercooled water, clouds, fog and precipitation,
- negative airframe temperature, which will be in the above-mentioned conditions [4, 5].

The icing phenomenon of an aircraft is a multi-factorial empirical process, and depends on:

- the size of water molecules in the atmosphere,
- atmospheric temperature,
- aircraft's flight velocity,
- the shape of the wing airfoil of the aircraft,
- the density of the medium, and thus the altitude of the flight of the aircraft,
- relative humidity of the medium [6].

The aircraft flight in icing conditions causes changes in airfoil shape. As a result of changing the shape of the airfoil, decreases the maximum value of the lift force coefficient C_L, and as a consequence the lift force F_L generated by the airfoil is reduced. The ice structures deposited on the airfoil also increase drag force F_D of the aircraft and the mass as a consequence the gravity force G [7, 8, 9].The aircraft flight in icing conditions increases the energy demand and fuel consumption of aircraft engines [10, 11, 12, 13].During the aircraft flight, the icing process of airfoil begins with the accumulation of ice on the nose surface of the airfoil within the stagnation point [14]. This article presents the results of CFD simulations research on analysis of thermodynamic parameters of air at the stagnation point of airfoil depending on the flight conditions of the aircraft in the aspect of identifying conditions conducive to the initiation of the icing process [15, 16, 17, 18, 19].

2 Methodology

A representative aircraft from the General Aviation category was selected as the test object. This choice was dictated by the operational properties of General Aviation aircraft and their exposure to conditions conducive to the phenomenon of icing of the airframe surface.The geometry of the wing model was based on the results of geometry measurements of the Cirrus SF50 Vision Jet wing (fig. 2). The measurements were made in three cross-sections of the wing, using a measuring gantry and a laser rangefinder. Measurements of the shape of the upper and lower surface of the wing made it possible to plot the actual wing airfoil of the Cirrus SF50 Vision Jet. A part of the lower surface of the wing was omitted during measurements due to difficulties associated with the chassis elements located there (fig. 3).

Fig. 2. Research object: Cirrus SF50 Vision Jet wing.

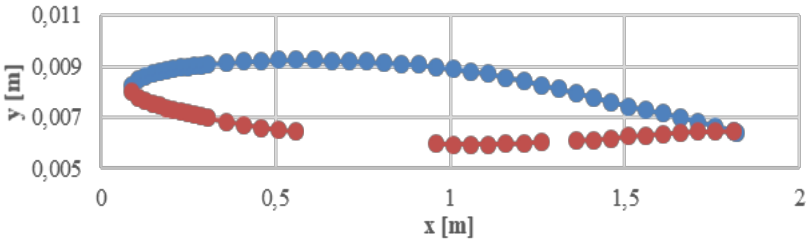

Fig. 3. The geometry of the Cirrus SF50 Vision Jet wing airfoil based on the measurements of the top and bottom surfaces of the wing.

The wing model were made in the SolidWorks environment (fig. 4). The characteristic dimensions of the wing are: the length of the wing L=5,4 [m], the root chord c_R=2 [m], the tip chord c_T= 1,4 [m], the taper ratio $\lambda=c_T/c_R$=0,7, the mean aerodynamic chord $c_M=2\cdot c_R\cdot(1+\lambda+\lambda^2)/(3\cdot(1+\lambda))$=1,718 [m], dihedral angle β=7,4°.

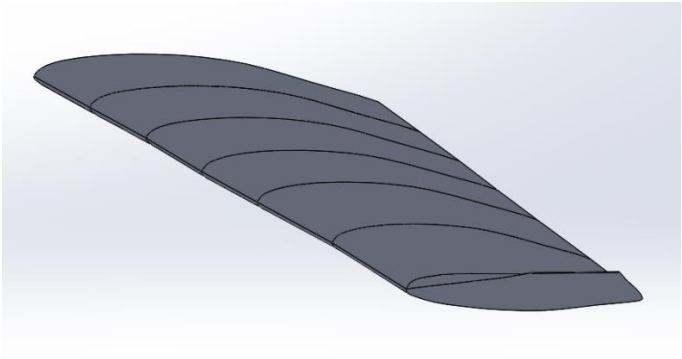

Fig. 4. Wing model for CFD tests: Cirrus SF50 Vision Jet wing model.

The mesh of the Cirrus SF50 Vision Jet wing model consists of 228 551 nodes, of which 223 510 are fluid nodes, and 5041 solid nodes (fig. 5).

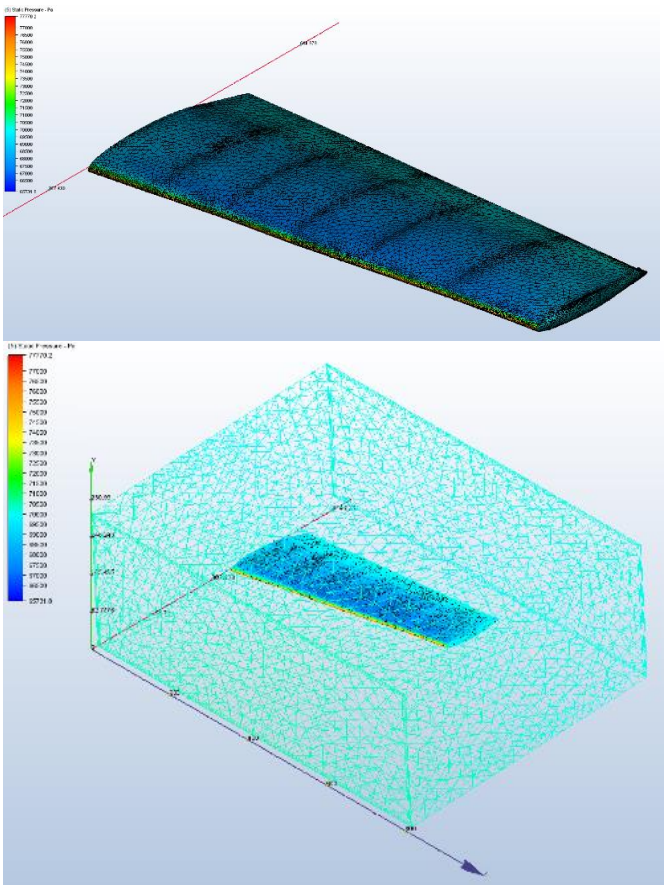

Fig. 5. The mesh of the Cirrus Vision Jet SF50 wing designed for CFD testing.

The numerical simulations were carried out in the AUTODESK CFD environment under standard atmosphere conditions for selected aircraft flight velocity. The CFD simulation

conditions are shown in table 1. CFD tests assumed a universal angle of attack α=4°. The simulation model used was the turbulent k-epsilon model for compressible gas.

Table 1. CFD simulation conditions for dry medium.

No.	Aircraft velocity	Flight altitude	Air temperature	Air pressure	Air density	Dynamic viscosity	Kinematic viscosity	Reynolds number
	v [m/s]	H [m]	T_A [K]	P_A [Pa]	ρ_A [kg/m^3]	μ [10^{-5} N·s/m^2]	ν [10^{-5} m^2/s]	Re=(c_M·v)/ν
1	40	0	288	101 325	1.225	1.789	1.460	4 706 849.32
2	50	0	288	101 325	1.225	1.789	1.460	5 883 561.64
3	60	0	288	101 325	1.225	1.789	1.460	7 060 273.97
4	70	0	288	101 325	1.225	1.789	1.460	8 236 986.30
5	80	0	288	101 325	1.225	1.789	1.460	9 413 698.63
6	40	1 000	282	89 867	1.112	1.758	1.581	4 346 616.07
7	50	1 000	282	89 867	1.112	1.758	1.581	5 433 270.08
8	60	1 000	282	89 867	1.112	1.758	1.581	6 519 924.10
9	70	1 000	282	89 867	1.112	1.758	1.581	7 606 578.12
10	80	1 000	282	89 867	1.112	1.758	1.581	8 693 232.13
11	40	3 000	269	70 089	0.909	1.694	1.864	3 686 695.28
12	50	3 000	269	70 089	0.909	1.694	1.864	4 608 369.10
13	60	3 000	269	70 089	0.909	1.694	1.864	5 530 042.92
14	70	3 000	269	70 089	0.909	1.694	1.864	6 451 716.74
15	80	3 000	269	70 089	0.909	1.694	1.864	7 373 390.56
16	40	5 000	256	53 994	0.736	1.628	2.212	3 106 690.78
17	50	5 000	256	53 994	0.736	1.628	2.212	3 883 363.47
18	60	5 000	256	53 994	0.736	1.628	2.212	4 660 036.17
19	70	5 000	256	53 994	0.736	1.628	2.212	5 436 708.86
20	80	5 000	256	53 994	0.736	1.628	2.212	6 213 381.56

The second stage of the research consisted in carrying out numerical simulations in the conditions presented in Table 1 with additional consideration of 5 selected values of relative air humidity φ [%] for subsequent settings φ = 20, 40, 60, 80, 100 [%]. In total, 120 numerical simulations of the SF50 wing model were performed in standard atmosphere conditions, taking into account the effect of relative air humidity φ.
The analysis of CFD tests results enabled the development of a model identifying the airfoil icing process beginning depending on the flight conditions of the aircraft. The area within the stagnation point was defined as a sphere with radius r=0.01 [m] in which n=500 measurements of selected thermodynamic parameters were made. The test results are presented as average values from n=500 measurements of thermodynamic parameters of air within the stagnation point (fig. 6).

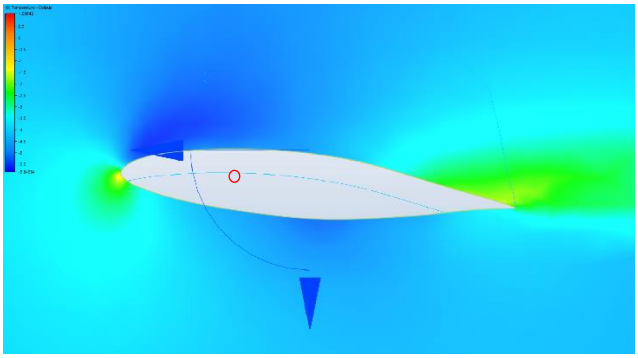

Fig. 6. The measurement area of thermodynamic parameters within the stagnation point.

3 Results

The change values of selected thermodynamic parameters within the stagnation point depending on the flight conditions of the aircraft in relation to the thermodynamic parameters of the dry medium determined on the basis of CFD tests are presented in table 2.

Table 2. Results of changes in thermodynamic parameters of the dry medium within the stagnation point based on CFD tests.

H [m]	v [m/s]	Δv [m/s]	ΔP [Pa]	ΔT [K]	Δρ [kg/m^3]
0	40	-28.563	1581.445	0.722	0.016
	50	-33.424	2129.816	1.098	0.021
	60	-40.750	3016.493	1.592	0.030
	70	-47.338	3951.999	2.165	0.038
	80	-55.056	5669.845	2.847	0.056
1000	40	-26.669	1388.004	0.702	0.014
	50	-32.833	1900.897	1.088	0.019
	60	-42.001	2906.795	1.618	0.029
	70	-48.653	3776.298	2.194	0.038
	80	-55.122	4999.518	2.858	0.050
3000	40	-27.635	1062.072	0.713	0.011
	50	-33.985	1589.327	1.106	0.017
	60	-42.771	2397.035	1.630	0.025
	70	-46.697	2961.791	2.147	0.031
	80	-55.484	4119.235	2.861	0.043
5000	40	-28.062	818.968	0.719	0.009
	50	-32.285	1209.897	1.076	0.013
	60	-41.791	1903.928	1.613	0.021
	70	-49.106	2486.188	2.200	0.027
	80	-56.024	3348.226	2.878	0.037

On the basis of the presented research results, a model was developed to determine the air temperature for dry medium within the stagnation point of the airfoil depending on the flight parameters of the aircraft: flight velocity v, flight altitude H and parameters of the International Standard Atmosphere (ISA). Dependence (1) presents the model in general, and the dependence (2) of the Cirrus SF50 Vision Jet wing airfoil.

$$T_{SP.dry} = \frac{P_A f(H) + \Delta P f(\mathrm{v}, H)}{(\rho_A f(H) + \Delta \rho f(\mathrm{v}, H)) \cdot R} \quad (1)$$

$$T_{SP.SF50.dry} = \frac{P_0 \cdot (1 - \frac{H}{44300})^{5,256} + ((-0{,}0073 \cdot H + 98{,}825) \cdot \mathrm{v} - (-0{,}1758 \cdot H + 2672{,}4))}{(\rho_0 \cdot (1 - \frac{H}{44300})^{4,256} + ((-6 \cdot 10^{-8} \cdot H + 0{,}001) \cdot \mathrm{v} - (-1 \cdot 10^{-6} \cdot H + 0{,}0254)) \cdot R} \quad (2)$$

where:

- T_{SP} – temperature within the airfoil stagnation point [K],
- $P_A f(H)$ – atmospheric air pressure as a function of altitude H based on the ISA standard atmosphere [Pa],
- $\Delta P f(\mathrm{v}, H)$ – pressure increase at the point of stagnation depending on the aircraft velocity v [m/s] and flight altitude H [Pa],
- $\rho_A f(H)$ – air density as a function of altitude H based on the ISA standard atmosphere [kg/m^3],
- $\Delta \rho f(\mathrm{v}, H)$ – air density increase at the point of stagnation depending on the aircraft velocity v and flight altitude H [kg/m^3],
- R – specific gas constant for dry air, R =286,9 [J/(kg·K)],
- P_0 – ambient pressure on standard mean sea level, P_0 =101 325 [Pa],
- ρ_0 – ambient density on standard mean sea level, ρ_0 =1,2255 [kg/m^3],
- H – aircraft flight altitude [m],
- v – aircraft velocity [m/s].

Analysis of the results of changes in moist air thermodynamic parameters within the stagnation point of the airfoil allowed to extend the determined model by the impact of relative air humidity and finally to develop a deterministic model of air temperature value changes ΔT within the airfoil stagnation point.

As a result of CFD numerical simulations, a database was obtained regarding the value of changes in moist air thermodynamic parameters within the airfoil stagnation point relative to the thermodynamic parameters of the medium:Δv [m/s], ΔP [Pa], ΔT [K], Δρ [kg/m^3]. Due to the large amount of data, only selected research results are presented in the article. Table 3 present examples of the results of thermodynamic parameter changes: ΔT [K], ΔP [Pa], Δρ [kg/m^3], and the values of the determined relative humidity coefficients, pressure and density correction values: φP, φρused in the general form of the moist air temperature model within the stagnation point of the airfoil depending on the flight parameters of the aircraft (3).

Table 3. Examples of the results of changes in thermodynamic parameters of the moist medium within the stagnation point based on CFD tests.

ΔT [K] for H=1000 [m]									
v [m/s]	40	50	60	70	80	90	100	φ [%]	
ΔT [K]	0.784	1.258	1.723	2.181	2.632	3.076	3.512	0	
	0.668	1.052	1.429	1.799	2.162	2.519	2.869	20	
	0.552	0.848	1.137	1.420	1.698	1.970	2.236	40	
	0.437	0.645	0.847	1.046	1.239	1.428	1.613	60	
	0.322	0.443	0.560	0.674	0.786	0.895	1.001	80	
	0.207	0.242	0.275	0.307	0.338	0.369	0.398	100	
ΔP [Pa] for H=1000 [m]									
v [m/s]	40	50	60	70	80	90	100	φ [%]	φP
ΔP [Pa]	1164.4	2079.65	2994.9	3910.15	4825.4	5740.65	6655.9	0	1
	1267.333	2263.491	3259.649	4255.807	5251.965	6248.123	7244.282	20	1.0884
	1370.266	2447.332	3524.398	4601.465	5678.531	6755.597	7832.663	40	1.1768
	1473.199	2631.173	3789.147	4947.122	6105.096	726.07	8421.045	60	1.2652
	1576.132	2815.014	4053.897	5292.779	6531.661	7770.544	9009.426	80	1.3536
	1679.0648	2998.8553	4318.6458	5638.4363	6958.2268	8278.017	9597.8078	100	1.442
Δρ [kg/m³] for H=1000 [m]									
v [m/s]	40	50	60	70	80	90	100	φ [%]	φρ
Δρ [kg/m³]	0.012	0.021	0.031	0.040	0.050	0.059	0.068	0	1
	0.014	0.024	0.035	0.046	0.057	0.067	0.078	20	1.1438
	0.015	0.028	0.040	0.052	0.064	0.076	0.088	40	1.2876
	0.017	0.031	0.044	0.058	0.071	0.084	0.098	60	1.4314
	0.019	0.034	0.049	0.063	0.078	0.093	0.108	80	1.5752
	0.021	0.037	0.053	0.069	0.085	0.101	0.118	100	1.719

$$T_{SP.humidity} = \frac{P_A f(H) + (\Delta P f(\mathrm{v}, H) \cdot \varphi \mathrm{P})}{(\rho_A f(H) + (\Delta \rho f(\mathrm{v}, H) \cdot \varphi\rho)) \cdot R} \tag{3}$$

Such a large database of air thermodynamic parameters values near the stagnation point of the airfoil depending on the flight parameters of the aircraft, determined correction coefficients for air pressure changes φP and air density changes φρ depending on the relative humidity of the air, and the use of model input data with the dependence(3) allowed to determine the functional dependencies necessary for the final development of a deterministic model of air temperature changes ΔT within the airfoil stagnation point depending on the flight altitude H [m], flight velocity v[m/s] and relative air humidity φ [%] for the aircraft wing of the Cirrus SF 50 Vision Jet (4).

$$\Delta T = (-4 \cdot 10^{-4} \cdot \varphi + (-5 \cdot 10^{-14} \cdot H^3 - 8 \cdot 10^{-11} \cdot H^2 + 3 \cdot 10^{-6} \cdot H + 0{,}0426)) \cdot v + \\ + (1 \cdot 10^{-10} \cdot H^2 + 6 \cdot 10^{-7} \cdot H + 0{,}0102) \cdot \varphi + (2 \cdot 10^{-8} \cdot H^2 - 2 \cdot 10^{-4} \cdot H - 0{,}4316) \quad (4)$$

where:

ΔT – air temperature change within the airfoil stagnation point relative to the air temperature of the medium at the current flight altitude of the aircraft,
φ – relative air humidity at the current flight altitude of the aircraft [%],
H – aircraft flight level [m],
v – aircraft flight velocity [m/s].

4 Conclusions

The results of CFD numerical simulation tests of the Cirrus SF 50 Vision Jet wing model developed on the basis of measurements of the real object geometry and their analysis in the form of searching for functional dependencies of changes in air thermodynamic parameters within the stagnation point of the airfoil in relation to the thermodynamic parameters of the medium allowed for the development estimation of the deterministic model of the magnitude of the change in the air temperature value within the stagnation point of the tested airfoil on the basis of the flight parameters of the aircraft such as: flight altitude H [m], flight velocity v [m/s] and relative air humidity φ [%].The estimation error between the values of the temperature increase ΔT determined during the CFD tests and the ΔT values estimated on the basis of the developed model does not exceed 5%. The developed model will be validated in the future on the basis of an experiment carried out in a wind tunnel. The model determined as part of the work allows estimating air temperature near the nose of the airfoil, which allows for reliable estimation of the risk of wing icing process beginning. The air temperature within the airfoil stagnation point less than 0 °C should be considered as conditions favorable for the icing process beginning. The developed model can be used as a diagnostic tool for prophylactic prevention of the phenomenon of aircraft wing icing.

References

1. A. Milkiewicz, R. Stepaniuk Praktyczna aerodynamika i mechanika lotu samolotu odrzutowego, w tym wysokomanewrowegoWydawnictwo Instytutu Technicznego Wojsk Lotniczych Warszawa (2009).
2. Gębura A Janusiak K and Paradowski M 2014 Oblodzenie statku powietrznego – przyczyny, skutki, przeciwdziałanie Journal of KONBiN, 4, 32 (2014).
3. Y. Liu, L.Q. Ma, W. Wang, A.K. Kota An experimental study on soft PDMS materials for aircraft icing mitigation. Applied Surface Science, 447 599−609 (2018).
4. P. Szewczak Meteorologia dla pilota samolotowego (PPL, CPL, ATPL, IR) Seria szkoleniowa „AVIA-TEST'' Poznań (2007).
5. L. Szutowski Poradnik pilota samolotowego Seria szkoleniowa „AVIA-TEST'' Poznań (2007).
6. J. Lewitowicz, A. Żyluk Podstawy eksploatacji statków powietrznych. Vol 5. Wydawnictwo Instytutu Technicznego Wojsk Lotniczych Warszawa (2006).
7. C. Antonini, M. Innocenti, T. Horn, M. Marengo, A. Amirfazli A Understanding the effect of superhydrophobic coatings on energy reduction in anti-icing systems. Cold Regions Science and Technology, 67, 1−2 (2011).

8. M.B. Bragg, G.M. Gregorek, J.D. Lee Airfoil aerodynamics in icing conditions Journal of Aircraft, 23, 1, 76−81 (1986).
9. J. Markowski Correction of the Model for Assessing the Emission of Harmful Exhaust Emissions from the Engine of a Small Aircraft During the Flight Transportation Research Procedia, 35 (2018).
10. J. Markowski, J. Pielecha, R. Jasiński Model to assess the exhaust emissions from the engine of a small aircraft during flight. Procedia Engineering, 192 (2017).
11. R. Jasiński, J. Markowski, J. Pielecha Probe positioning for the exhaust emissions measurementsProcedia Engineering, 192 (2017).
12. R. Jasiński, J. Pielecha, J. Markowski Emission of particulate matter during aircraft landing operation. MATEC Web of Conferences, 10, (2016).
13. G. Fortin, J.L. Laforte, A. Ilinca Heat and mass transfer during ice accretion on aircraft wings with an improved roughness model International Journal of Thermal Sciences, 45, 6, 595−606 (2006).
14. R. Chachurski, P. Waślicki Wykrywanie i sygnalizacja oblodzenia statków powietrznych. Prace Instytutu Lotnictwa 213 Warszawa (2011).
15. J. Chen, J. Liu, M. He, K.Y. Li, D.P. Cui, Q.L. Zhang, X.P. Zeng, Y.F. Zhang, J.J. Wang, Y.L. Song Superhydrophobic surfaces cannot reduce ice adhesion. Applied Physics Letters, 101, 11, 111603 (2012).
16. L. Pfitzenmaier, C.M.H. Unal, Y. Dufournet, H.W.J. Russchenberg Observing ice particle growth along fall streaks in mixed-phase clouds using spectral polarimetric radar dat.a Atmospheric Chemistry and Physics, 18, 11, 7843−7862 (2018).
17. J.R. Raol, J. Singh Flight mechanics modeling and analysis CRC Press Tay-lor & Francis Group Boca Raton (2009).
18. L. Smith, K.J. Craig, J.P. Meyer, G.R. Spedding Numerical investigation of the aerodynamic performance for an alternative wing-body-tail configuration. Journal of Aircraft, 56, 1, 250−261 (2019).